  Bull. Chem. Soc. Jpn., 57, 3300—3306 (1984) [Vol. 57, No. 11

Polarized Raman and Phosphorescence Spectra of [$^1H_4$]- and [$^2H_4$]Pyrimidines

Masayuki UMEMOTO,† Taketora OGATA,†† Hiroko SHIMADA,†† and Ryoichi SHIMADA*

†*Yamaguchi Prefectural Environmental Pollution Research Center, Hiruta, Asada, Yamaguchi 753*

††*Department of Chemistry, Faculty of Science, Fukuoka University, Nanakuma, Jonan-ku, Fukuoka 814*

Department of Chemistry, Faculty of Science, Kyushu University, 33, Hakozaki, Higashi-ku, Fukuoka 812

(Received June 21, 1984)

Assignments of the out-of-plane normal vibrations of [$^1H_4$]- and [$^2H_4$]pyrimidines were reexamined through studies of the polarized Raman, time-resolved phosphorescence and polarized dark sublevel phosphorescence spectra. The vibrational analyses of the phosphorescence spectra based on their polarization behavior indicate that the appearance of the strong 0-0 and totally symmetric vibronic bands in the dark sublevel phosphorescence spectra is attributed to the distortion of the molecular structure along the b_1 normal coordinates in the lowest triplet state.

The phosphorescence spectrum of pyrimidine has been studied by many workers and the emitting triplet state of this molecule was assigned to $^3B_1$ (n, π^*).[1-4] Nishi *et al.*[5] observed the phosphorescence spectrum at 4.2 K and pointed out that the 0-0 and totally symmetric vibronic bands arise from the T_z (B_2) and T_y (A_1) sublevels of the lowest triplet state, while the out-of-plane vibronic bands arise, very likely, from the dark T_x (A_2) sublevel, where the x and z axes were taken as the direction normal to the molecular plane and the C_2 axis, respectively. Chan and Sharnoff[6] determined the ordering of the sublevels of the lowest triplet state in pyrimidine to be T_x, T_y, and T_z using the microwave optical double-resonance technique. Burland and Schmidt[7] investigated the dynamic behavior of the pyrimidine molecule in the lowest triplet state using the microwave-induced delayed phosphorescence technique and pointed out that the populating rate for the T_x sublevel was unexpectedly high. Recently, Inoue and Lim[8] observed the zero-field electron paramagnetic resonance transitions among the sublevels of the lowest triplet state of pyrimidine in a benzene host crystal at 1.6 K by the optical detection of the resonance transitions and suggested that the unusually high T_x population is associated with the pseudo-Jahn-Teller distortions of the potential surfaces in the $^3A_1$ (π, π^*) and $^3B_2$ (π, π^*) states perturbed by a close-lying $^3A_2$ (n, π^*) state.

In this paper, the vibrational analyses of the phosphorescence spectra of [$^1H_4$]- and [$^2H_4$]pyrimidines will be reexamined through the studies of the polarized T_x sublevel phosphorescence spectra in benzene host crystals and the polarized Raman spectra in single crystals. The molecular structure in the lowest triplet state will be also discussed.

Experimental

Chemicals. [$^1H_4$]Pyrimidine, obtained from Nakarai Chemicals, was purified by repeated distillation under reduced pressure. [$^2H_4$]Pyrimidine, which was kindly supplied by Professor Lionel Goodman of Rutgers University, was purified by vacuum distillation. Methylcyclohexane and benzene of Dotite Spectrosol Grade were used without further purification.

Optical Measurements. The time-resolved phosphorescence spectra and the phosphorescence lifetimes of [$^1H_4$]- and [$^2H_4$]pyrimidines were studied in methylcyclohexane and benzene matrices at various temperatures between 4.2 and 1.4 K. Liquid helium in the Dewar vessel, where the sample was held, was pumped out with a rotary pump of 1000 L min^{-1} displacement, and the sample was kept at desired temperatures by controlling the speed of evacuation of helium gas with a valve placed between the pump and the Dewar vessel. The temperature of the sample was determined by measuring the vapor pressure of helium in the top of the Dewar vessel. The short-lifetime phosphorescence was observed in the following way. The sample was excited for 10 ms. Two ms after the excitation ceased, the phosphorescence was sampled for 10 ms. The long-lifetime phosphorescence was observed at exciting, waiting, and sampling times of 200, 200, and 200 ms, respectively.

The polarized long-lifetime phosphorescence spectra were observed in a benzene host crystal at 1.4 K. The single-crystal specimen was obtained as follows. Single crystals of benzene doped with [$^1H_4$]- and [$^2H_4$]pyrimidines, were made by the Bridgman method at low temperature. Well grown single crystals examined under polarized light were cut about 2 mm in thickness along a cleavage plane with a razor blade in a cold room kept at −15 °C and suspended in an inner Dewar vessel precooled to −30 °C. Liquid nitrogen was poured into an outer Dewar vessel and the Dewar vessels were allowed to stand for about 10 h. Then, after pouring liquid helium very gradually into the inner Dewar vessel, the samples were examined again under polarized light. Only the crystals which were not cracked were used for the measurement of the polarized spectrum. Since we had no crystallographic knowledge about the cleavage plane cut out from the benzene single crystal, the polarized phosphorescence spectrum was observed with a rotatable polarizer whose orientation was set in such a way that the intensity of the 0-0 band of the long-lifetime phosphorescence spectrum became the strongest and the rotation of the polarizer by 90° gave the weakest intensity. The spectra observed at the former and latter orientations of the polarizer are drawn with solid and dotted lines (referred to as A and B spectra, respectively). The optical and electronic arrangements used for the measurements of the time-resolved phosphorescence spectrum, the polarized phosphorescence spectrum and the phosphorescence lifetimes are exactly the same as those described previously.[9,10]

The polarized Raman spectra of [$^1H_4$]- and [$^2H_4$]pyrimidine single crystals were observed at −30 °C in the crystal orientation where the Raman bands observed at 395 cm^{-1} for [$^1H_4$]-pyrimidine and at 365 cm^{-1} for [$^2H_4$]pyrimidine showed drastic change of polarization behavior by rotating the polarizer under the same way as described previously.[11]

The Raman spectrum polarized parallel to the crystal growth direction is referred to as // spectrum and the spectrum polarized perpendicular to as ⊥ spectrum.

Results and discussion

Out-of-plane Normal Vibrations. Although the normal vibrations of [$^1H_4$]- and [$^2H_4$]pyrimidines have been studied by many workers,[12–15] the assignments given for the normal vibrations, especially for the out-of-plane vibrations, do not agree with each other. Therefore, the out-of-plane vibrations were reexamined by studing the polarized Raman spectrum and normal coordinate calculations. The normal coordinate calculation for the out-of-plane vibrations was carried out with a valence force field and the ϕ-type torsional coordinate using the same method as described previously.[16] Values of the force constants are given in Table 1, where the notations Q, q, P, p, and t are the same as those given by Whiffen.[17] Calculated vibrational frequencies and modes for [$^1H_4$]- and [$^2H_4$]pyrimidines are listed in Tables 2 and 3, respectively.

The polarized Raman spectra of [$^1H_4$]- and [$^2H_4$]-pyrimidines are shown in Fig. 1. As can be seen in this figure, the non-totally symmetric Raman bands, which are depolarized in molten phase, are classified into three types (I, II, and III) based on their polarization behavior. In the first type, the intensity of the ⊥ band is stronger than that of the // band. In the second type, the intensity of the // band is stronger than that of the ⊥ band, and in the third type the intensity of the ⊥ band is much stronger than that of the // band. A comparison of the polarization behavior of the Raman bands with the band contours of the corresponding infrared bands observed in a vapor phase[12] indicates that the type-I and-II Raman bands should be assigned to vibrations belonging to b_2 and b_1 symmetry species, respectively. Hence, the type-III Raman bands are assigned to a_2 species.

Table 1. Force constants for out-of-plane vibrations

$Q_{C'-N}$	0.17
Q_{C-N}	0.18
Q_{C-C}	0.20
q^o	−0.06
q^m	0.03
$P_{H'}$	0.31
P_H	0.34
p^o	0.07
$p^m_{H,H'}$	−0.05
$p^m_{H,H}$	−0.07
p^p	0.02
$t^o_{C'-N,H'}$	−0.04
$t^o_{C-N,H}$	−0.02
$t^o_{C-C,H}$	−0.02

[in aNmrad^{-2}(=mdyn Å/rad^2)units]

C′ is the carbon atom placed between the two N atoms.
H′ is the hydrogen atom bonded to the C′ atom.

The Raman bands of [$^1H_4$]pyrimidine observed at 345, 725, 775, and 982 cm^{-1} showed type-II polarization behavior and, thus, these were assigned to the ν_{16b}, ν_{11}, ν_4, and ν_{17b} vibrations of b_1 species, respectively. The vibrational modes were determined based on the normal coordinate calculation and also through the analysis of the phosphorescence spectrum. The bands observed at 395 and 1004 cm^{-1} showed type-III polarization and, thus, they were assigned to the ν_{16a} and ν_{17a} vibrations of a_2 species, respectively. The Raman bands of [$^2H_4$]pyrimidine observed at 300, 553, 675, 720, and 850 cm^{-1} showed type-II polarization behavior and the bands at 365 and 807 cm^{-1} showed type-III polarization. Thus, the former were assigned to the ν_{16b}, ν_{11}, ν_{10b}, ν_4, and ν_{17b} vibrations and the latter to the ν_{16a} and ν_{17a} vibrations, respectively. The ν_{10b} vibration of [$^1H_4$]pyrimidine could not be identified in the polarized Raman spectrum. The out-of-plane normal vibrations thus assigned are given in Tables 2 and 3, together with those given by previous workers.[12–15] Our assignments explain well the observed polarization behavior of the phosphorescence spectra (described later).

Phosphorescence Spectrum. The temperature dependence of the relative intensities of the ν_{17b}, ν_{11}, and ν_{16b} bands with respect to the 0-0 band in the long-lifetime phosphorescence and that of the lifetime of the long-lifetime phosphorescence observed in methylcyclohexane are shown in Figs. 2 and 3, respectively. As can be seen in these figures, the relative intensity and the lifetime became almost

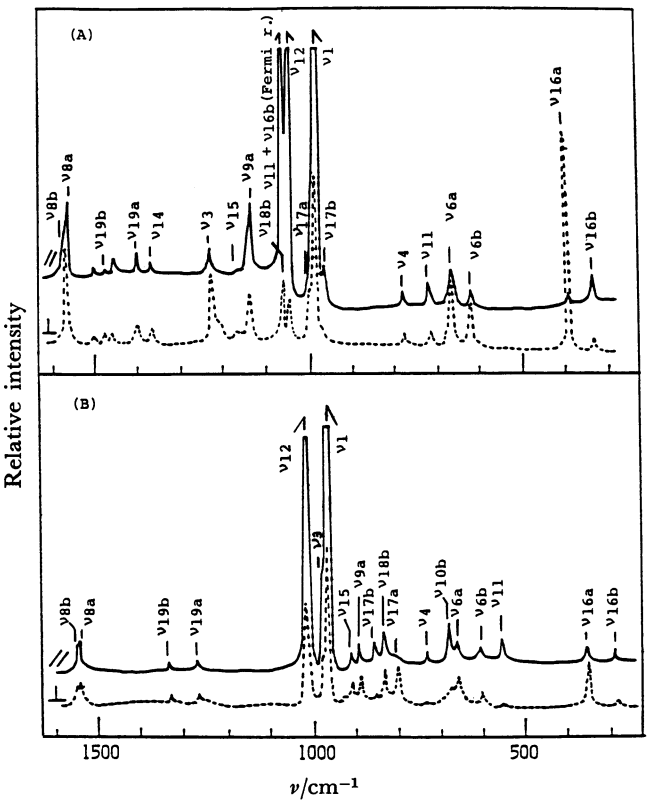

Fig. 1. Polarized Raman spectra of [$^1H_4$]-(A) and [$^2H_4$]pyrimidine (B) single crystals.

TABLE 2. OUT-OF-PLANE VIBRATIONS OF [$^1H_4$]PYRIMIDINE

Sym. Spec.	Mode	Sbrana[12]	Foglizzo[13]	Milani[14] -Nejad	Bokobza[15] -Sebagh	This work			
						Raman	Calcd	Phosphorescence in Mc[b]	Phosphorescence in Bz[b]
		$\tilde{\nu}$/cm^{-1}	$\tilde{\nu}$/cm^{-1}	$\tilde{\nu}$/cm^{-1}	$\tilde{\nu}$/cm^{-1}	$\tilde{\nu}$/cm^{-1}	$\tilde{\nu}$/cm^{-1}	$\tilde{\nu}$/cm^{-1}	$\tilde{\nu}$/cm^{-1}
a_2	ν_{17a}	870			927	1004	994	1005	1002
	ν_{16a}	394	393	398.5	398	395	395	392	405
b_1	ν_{17b}[a]	993	981	980	980	982	993	962	969
	ν_{10b}	719	829	721	955		861	804	820
	ν_{11}	804	720	811	810	725	723	716	732
	ν_4	709	717	708	720	775	770		
	ν_{16b}	344	344	344	346	345	354	339	349

a) Previous workers[12-15] gave ν_5 mode for this vibration. b) Mc=methylcyclohexane, Bz=benzene.

TABLE 3. OUT-OF-PLANE VIBRATIONS OF [$^2H_4$]PYRIMIDINE

Sym. spec.	Mode	Sbrana[12]	Milani[14] -Nejad	This work			
				Raman	Calcd	Phosphorescence in Mc	Phosphorescence in Bz
		$\tilde{\nu}$/cm^{-1}	$\tilde{\nu}$/cm^{-1}	$\tilde{\nu}$/cm^{-1}	$\tilde{\nu}$/cm^{-1}	$\tilde{\nu}$/cm^{-1}	$\tilde{\nu}$/cm^{-1}
a_2	ν_{17a}		801	807	818	800	811
	ν_{16a}		369	365	360	374	371
b_1	ν_{17b}[a]	848	820	850	857	833	840
	ν_{10b}	552	561	675	662	669	675
	ν_{11}	669	669	553	545	556	560
	ν_4		553	720	714		716
	ν_{16b}	304	304	300	303		

a) Previous workers[12,14] gave ν_5 mode for this vibration.

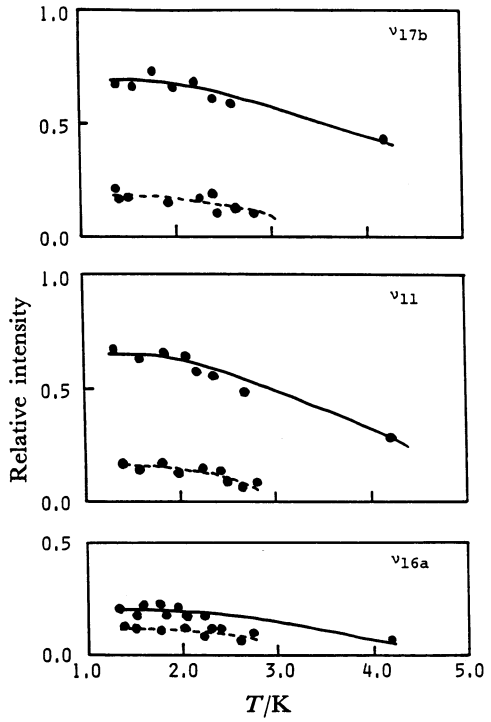

Fig. 2. Temperature dependence of the relative intensities of the ν_{17b}, ν_{11}, and ν_{16a} bands to the 0-0 band in the long-lifetime phosphorescences of [$^1H_4$]-(——) and [$^2H_4$]pyrimidins (----).

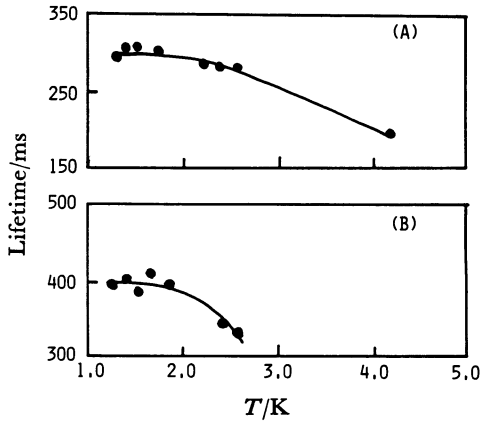

Fig. 3. Temperature dependence of the lifetimes of the long-lifetime phosphorescences of [$^1H_4$]-(A) and [$^2H_4$]pyrimidines (B).

constant at temperatures below 2 K. This indicates that the spin lattice relaxation, involving the dark T_x sublevel of the lowest triplet state, hardly takes place at temperatures below 2 K within the lifetime of the T_x sublevel. Thus, one can conclude that the long-lifetime phosphorescence observed at 1.4 K arises directly from the T_x sublevel.

The lifetimes of the lowest triplet sublevels at 1.4 K are given in Table 4, together with the values measured by Burland and Schmidt.[7] The lifetime of the T_x sub-

Table 4. Phosphorescence lifetimes of [$^1H_4$]- and [$^2H_4$]pyrimidines

	[$^1H_4$]Pyrimidine			[$^2H_4$]Pyrimidine		
	Burland[7] (1.2 K)	This work (1.4 K)		Burland[7] (1.2 K)	This work (1.4 K)	
	in Bz	in Bz	in Mc	in Bz	in Bz	in Mc
T_x	324	330	310	465	440	400
T_y	16.6			17.8		
		15	13		20	15
T_z	11.8			13.0		

(in ms units)

level is so long compared with those of the T_y and T_z sublevels that the long-lifetime phosphorescence spectrum can easily be separated out from the short-lifetime T_y and T_z spectra. While the T_z sublevel spectrum could not be separated from the T_y spectrum under our experimental technique due to very close lifetimes of these two sublevels.

The time-resolved phosphorescence spectra of [$^1H_4$]- and [$^2H_4$]pyrimidines observed in methylcyclohexane matrix at 1.4 K are shown in Figs. 4 and 5, respectively. Intensity ratio of the 0-0 bands of the "long-" and "short-" lifetime spectra extrapolated at t=0 ms, that is, when the excitation light was cut off, was determined to be about 1/100. The

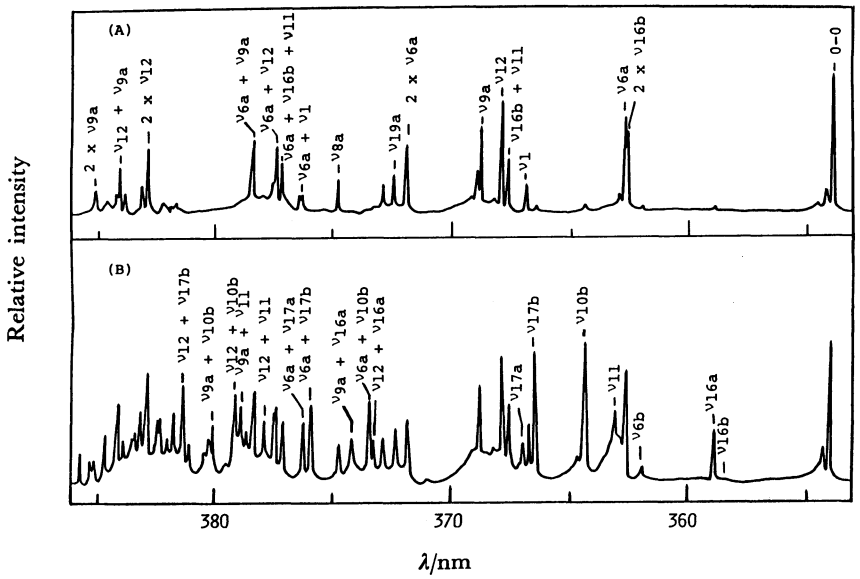

Fig. 4. Short (A) and long (B) lifetime phosphorescence spectra of [$^1H_4$]pyrimidine in methylcyclohexane at 1.4 K.

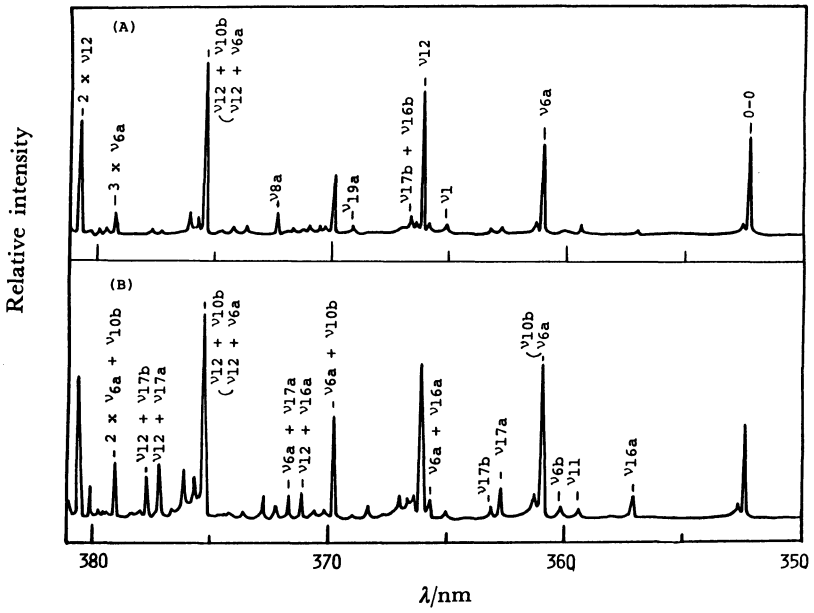

Fig. 5. Short (A) and long (B) lifetime phosphorescence spectra of [$^2H_4$]pyrimidine in methylcyclohexane at 1.4 K.

spectra shown in Figs. 4 and 5 were drawn after the observed intensities of the 0-0 bands in both the spectra were normalized to unity. Vibrational analysis made on the appreciably intense bands in the short-lifetime phosphorescence spectrum was the same as that given by Nishi *et al.*[5] and Hochstrasser and Marzzacco[18] for the phosphorescence spectrum observed at 4.2 K. Although the long-lifetime phosphorescence gave essentially the same spectral structure as that of the short-lifetime phosphorescence, the most characteristic feature of the long-lifetime spectrum was a remarkable increase of the relative intensities of some vibronic bands with respect to the 0-0 band.

The short-and long-lifetime phosphorescence spectra observed in a benzene matrix at 1.4 K showed essentially the same spectral structure as those observed in methylcyclohexane. The polarized long-lifetime phosphorescence spectra of [$^1H_4$]- and [$^2H_4$]-pyrimidines doped in a benzene host single crystal are given in Figs. 6 and 7, respectively. The bands in the polarized phosphorescence spectrum can be classified into two types. In the first type, the intensity of the A spectrum is stronger than that of the B spectrum while in the second type the intensity relation is *vice versa*. Based on the polarization behavior of the bands, vibrational analyses of the phosphorescence spectra of [$^1H_4$]- and [$^2H_4$]pyrimidines were carried out.

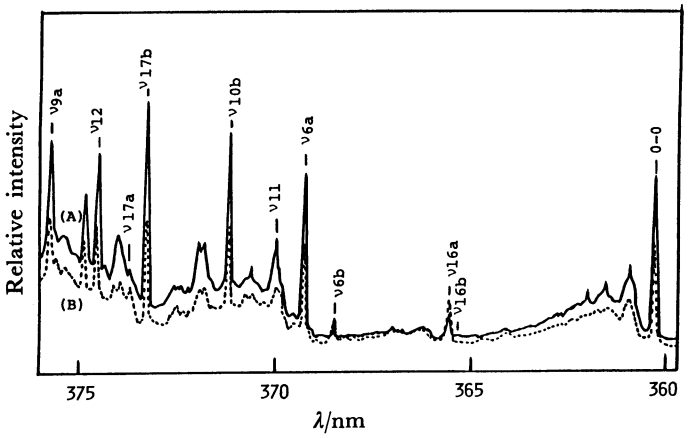

Fig. 6. Polarized long-lifetime phosphorescence spectrum of [$^1H_4$]pyrimidine in benzene host crystal at 1.4 K. A and B are referred to the paper.

[$^1H_4$]Pyrimidine: The phosphorescence bands separated by 392, 618, 716, 804, 962, 1005, 1465, 1484, 1533, 1646, 1795, 1861, 1876, 1940, and 2030 cm^{-1} from the 0-0 band are much intensified relative to the 0-0 band in the long-lifetime spectrum compared with the short-lifetime spectrum. Among them the 392, 618, 1005, 1465, and 1533 cm^{-1} bands showed the second-type polarization behavior in the polarized long-lifetime phosphorescence spectrum, while the other showed the first-type polarization. By referring the polarized Raman spectrum and the normal coordinate calculation, 392, 618, 716, 804, 962, and 1005 cm^{-1} bands were assigned to the ν_{16a}, ν_{6b}, ν_{11}, ν_{10b}, ν_{17b}, and ν_{17a} vibrations, respectively. Hence, it is concluded that the intensified bands showing the first-type polarization behavior can be assigned to the b_1 vibronic bands, while those showing the second-type polarization to the a_2 or b_2 bands. The other intensified bands were assigned to combination bands involving these out-of-plane vibrations based on their polarization behaviors. Generally, the H wagging vibrations are the most effective for the vibronic coupling between (n, π^*) and (π, π^*) states and thus the H wagging vibrations are expected to be observed with fairly strong intensity in the dark sublevel phosphorescence spectrum. Therefore, intensified bands in the dark T_x sublevel phosphorescence spectrum could be assigned to the H wagging vibrations. Our assignment given for the modes of the out-of-plane vibrations were made based on this point.

[$^2H_4$]Pyrimidine: The phosphorescence bands separated by 374, 556, 608, 669, 800, 833, 1029, 1323, 1421, 1465, 1720, and 1857 cm^{-1} from the 0-0 band in methylcyclohexane are intensified relative to the 0-0 band in the long-lifetime spectrum. Among them the 374, 608, 800, 1029, 1421, 1465, and 1857 cm^{-1} bands showed the second-type polarization behavior in the polarized phosphorescence spectrum and the

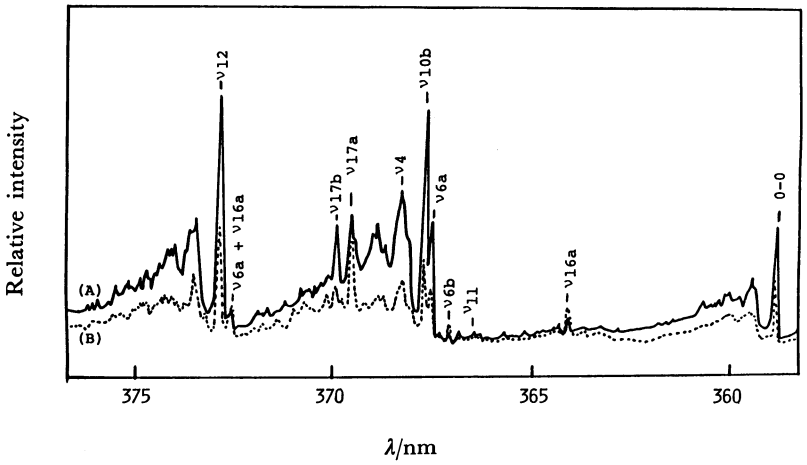

Fig. 7. Polarized long-lifetime phosphorescence spectrum of [$^2H_4$]pyrimidine in benzene host crystal at 1.4 K.

others showed the first-type polarization. The 374, 608, and 800 cm^{-1} bands were assigned to the ν_{16a}, ν_{6b}, and ν_{17a} vibrations, respectively, and the 556, 669, and 833 cm^{-1} bands to the ν_{11}, ν_{10b}, and ν_{17b} vibrations, respectively, by referring Table 3. As in the case of [$^1H_4$]pyrimidine, the first-type polarization behavior in the phosphorescence spectrum is attributed to the b_1 vibronic bands and the second type to the a_2 or b_2 bands. It should be noted that the 0-0 and totally symmetric vibronic bands showed the first type, that is, b_1 polarization behavior in the long-lifetime phosphorescence spectra of [$^1H_4$]- and [$^2H_4$]pyrimidines as can be seen in Figs. 6 and 7. Detailed vibrational analyses are given in Figs. 4 and 5.

Molecular Structure in the Lowest Triplet State. It is quite impossible that the a_1 and b_1, and also a_2 and b_2 vibronic bands show the same polarization behavior, respectively, so far as the molecular geometry of pyrimidine keeps the point group C_{2v} in the lowest triplet state even if the pyrimidine molecules take any orientations in a benzene host crystal. We will now discuss the orientation of the pyrimidine molecule in a benzene host single crystal. Hong and Robinson[19] observed two spectral origins in the phosphorescence of pyrazine in a benzene host crystal, where one is much stronger than the other, and suggested that most of the pyrazine molecules preferentially occupy the substitutional site of the host crystal with a certain fixed orientation. Since the molecular structure of pyrimidine is similar to that of pyrazine and the phosphorescence spectrum in a benzene host crystal shows single origin and distinct polarization behavior as can be seen in Figs. 6 and 7, it is believed that almost all pyrimidine molecules are oriented in a single way in a benzene host crystal. If the pyrimidine molecule, which belongs to the point group C_{2v}, deforms along the normal coordinates of a_2 symmetry species, the molecular symmetry reduces to the point group C_2 and thus a_1 and a_2 symmetry species go into a species, and b_1 and b_2 species into b species. On the other hand, if the molecule deforms along the b_1 normal coordinates the molecular symmetry reduces to the point group C_s, where the plane perpendicular to the original molecular plane and involving the z axis is the symmetry plane. In this case, a_1 and b_1 symmetry species go over into a′ species, and a_2 and b_2 species into a″ species. Thus the symmetrically forbidden transition in the C_{2v} molecular geometry becomes allowed if the molecular structure deforms to the point group C_2 or C_s.

The transitions from the T_x sublevel in the lowest triplet state to the totally symmetric vibrational levels in the ground state are strictly forbidden when the molecule has the C_{2v} geometry, while the transitions become allowed with z-polarization when the molecule deforms along the a_2 normal coordinates. In this case, the transitions from the T_x sublevel to the b_1 and b_2 vibrational levels of the ground state have x- and/or y-polarization, while transitions to the a_1 and a_2 levels have z-polarization. On the other hand, if the molecule deforms along the b_1 normal coordinates, the transitions from the T_x sublevel to the a_1 and b_1 vibrational levels have y-polarization, while the transitions from the T_x sublevel to the a_2 and b_2 levels have x- and/or z-polarization. These polarization behaviors are illustrated in Fig. 8.

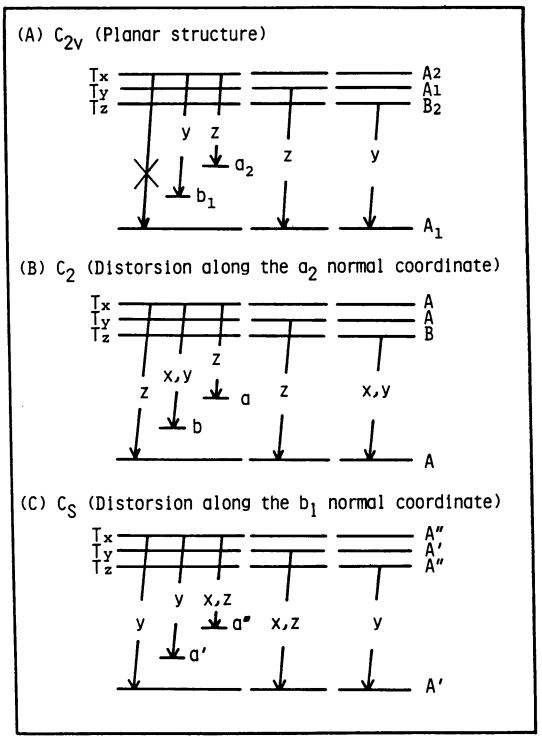

Fig. 8. Polarization directions of the phosphorescence bands emitted from each sublevels of the lowest triplet state in C_{2v} molecular geometry (A), in C_2 geometry (B), and in C_s geometry (C).

Since the 0-0 and totally symmetric vibronic bands show the same polarization behavior as that of the b_1 vibronic bands, as described above, one can understand that the direction of the transition moments of the 0-0 and totally symmetric vibronic bands coincide with that of the b_1 vibronic bands. Thus, one could conclude that the appearance of the 0-0 and totally symmetric bands in the long-lifetime phosphorescence spectrum is responsible for the molecular distortion along the b_1 normal coordinates in the lowest triplet state. This conclusion was supported by the fact that the b_2 and a_2 vibronic bands showed the same polarization behavior in the polarized long-lifetime phosphorescence spectrum, as described above.

We would like to express our thanks to Mr. Shoji Kizuki for his great help in the experiment. The present work was partially supported by a Grant-in-Aid for Scientific Research from the Ministry of Education, Science and Culture (No. 57470013).

References

1) R. Shimada, *Spectrochim. Acta*, **17**, 30 (1961).
2) V. G. Krishna and L. Goodman, *J. Am. Chem. Soc.*, **83**, 2042 (1961).
3) L. Goodman and R. W. Harrell, *J. Chem. Phys.*, **30**, 1131 (1959).
4) V. G. Krishna and L. Goodman, *J. Chem. Phys.*, **36**, 2217 (1962).
5) N. Nishi, R. Shimada, and Y. Kanda, *Bull. Chem. Soc.*

Jpn., **43**, 41 (1970).
6) Y. Chan and M. Sharnoff, *J. Lumin*, **3**, 155 (1970).
7) D. M. Burland and J. Schmidt, *Mol. Phys.*, **22**, 19 (1971).
8) A. Inoue and E. C. Lim, *Chem. Phys. Lett*, **62**, 250 (1979).
9) Y. Urabe, T. Watanabe, Y. Ishibashi, H. Shimada, and R. Shimada, *Mem. Fac. Sci. Kyushu Univ. Ser. C*, **13**, 1 (1981).
10) T. Watanabe, H. Shimada, and R. Shimada, *Bull. Chem. Soc. Jpn.*, **55**, 2564 (1982).
11) Y. Ishibashi, F. Arakawa, H. Shimada, and R. Shimada, *Bull. Chem. Soc. Jpn.*, **56**, 1327 (1983).
12) G. Sbrana, G. Adembri, and S. Califano, *Spectrochim. Acta*, **22**, 1831 (1966).
13) R. Foglizzo and A. Novak, *J. Chim. Phys.*, **64**, 1484 (1967).
14) F. Milani-Nejad and H. D. Stidham, *Spectrochim. Acta, Part A*, **31**, 1433 (1975).
15) L. Bokobza-Sebagh and J. Zarenbowitch, *Spectrochim. Acta, Part A*, **32**, 797 (1976).
16) Y. Ishibashi, R. Shimada, and H. Shimada, *Bull. Chem. Soc. Jpn.*, **55**, 2765 (1982).
17) D. H. Whiffen, *Philos. Trans. R. Soc. London, Ser A*, **248**, 131 (1955).
18) R. M. Hochstrasser and C. J. Marzzacco, *J. Mol. Spectrosc.*, **42**, 75 (1972).
19) H. K. Hong and G. W. Robinson, *J. Mol. Spectrosc.*, **42**, 75 (1972).